

Electronic Supplementary Information

Dual Role Far Red Fluorescent Molecular Rotor for Decoding the Plasma Membrane and Mitochondrial Viscosity

Akshay Silswal,^a Anup Pramanik^b and Apurba Lal Koner*^a

^a Department of Chemistry, Indian Institute of Science Education and Research Bhopal, Bhopal Bypass Road, Bhauri, Bhopal, Madhya Pradesh-462066, India. E-mail: akoner@iiserb.ac.in;

^b Department of Chemistry, Sidho-Kanho-Birsha University, Purulia, West Bengal-723104, India.

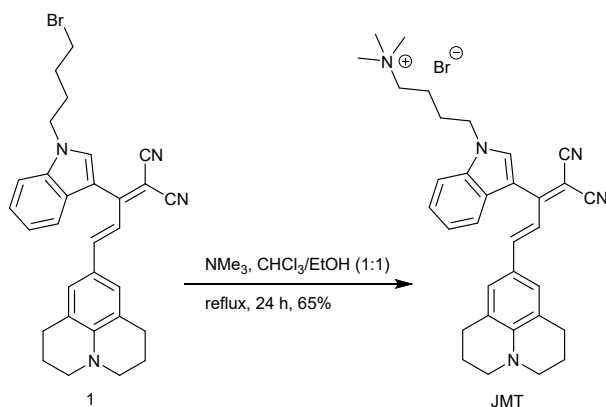
Table of Contents

S. No.	Contents	Page No.
1.	Synthesis and characterization	2-4
2.	Photophysical and Computed properties	5-7
3.	Cytotoxicity and live cell imaging	8-15
4.	References	15

Synthesis and characterization

Synthetic Scheme:

(*E*)-4-(3-(1,1-dicyano-4-(2,3,6,7-tetrahydro-1H,5H-pyrido[3,2,1-ij]quinolin-9-yl)buta-1,3-dien-2-yl)-1H-indol-1-yl)-*N,N,N*-trimethylbutan-1-aminium bromide (JMT):



Procedure:

Compound **1** was prepared as reported.¹

Compound **1** (120 mg, 0.22 mmol) was taken in a microwave vial and dissolved in ethanol/chloroform (1:1, 2 mL each) mixture. Then trimethylamine (540 μL , 2.2 mmol) was added and refluxed for 24 h. After completion, the solvent was evaporated, and the product was purified using column chromatography using neutral alumina gel and 0.5 \rightarrow 2.5% MeOH/DCM as eluent to obtain a brick red solid with a 65% yield.

^1H NMR (500 MHz, CD_3OD) δ 7.87 (s, 1H), 7.63 (d, $J = 8.3$ Hz, 1H), 7.47 (d, $J = 7.9$ Hz, 1H), 7.33 (t, $J = 7.5$ Hz, 1H), 7.28 (d, $J = 15.0$ Hz, 1H), 7.18 (t, $J = 7.5$ Hz, 1H), 7.10 (d, $J = 15.0$ Hz, 1H), 6.95 (s, 2H), 4.48 (t, $J = 6.0$ Hz, 2H), 3.33 – 3.26 (m, 6H), 3.06 (s, 9H), 2.77 – 2.60 (m, 4H), 2.02 – 1.97 (m, $J = 14.1, 7.0$ Hz, 2H), 1.96 – 1.89 (m, $J = 16.9, 11.7$ Hz, 4H), 1.83 – 1.74 (m, 2H).

$^{13}\text{C}\{^1\text{H}\}$ NMR (126 MHz, CD_3OD) δ 165.05, 150.72, 146.58, 136.54, 132.17, 128.70, 127.02, 122.74, 121.33, 121.24, 121.09, 120.52, 116.86, 115.56, 110.34, 109.01, 69.78, 65.82, 52.17, 49.68, 45.74, 27.22, 25.95, 21.07, 20.23.

HRMS (ESI) m/z $[\text{M}]^+$ calculated mass- 504.3122 Da obtained mass- 504.3159 Da

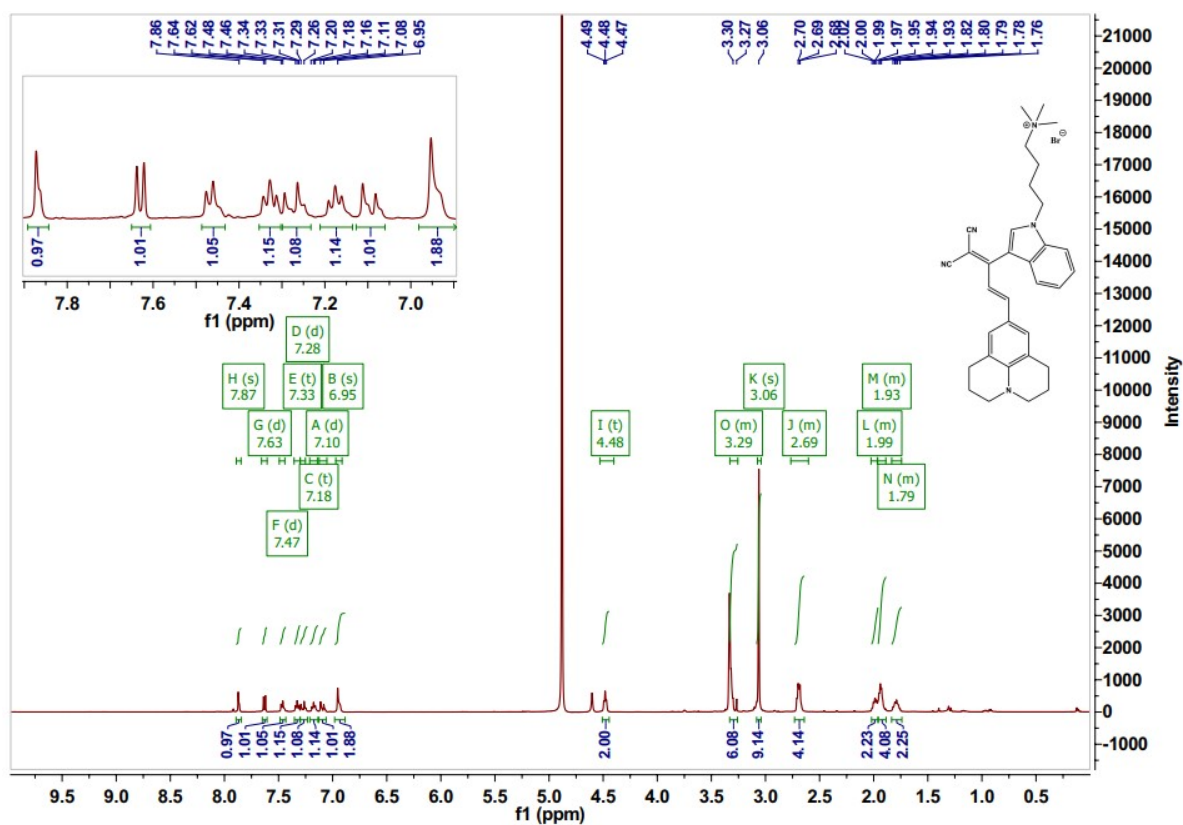


Fig. S1 ^1H NMR spectrum of compound **JMT** in CD_3OD

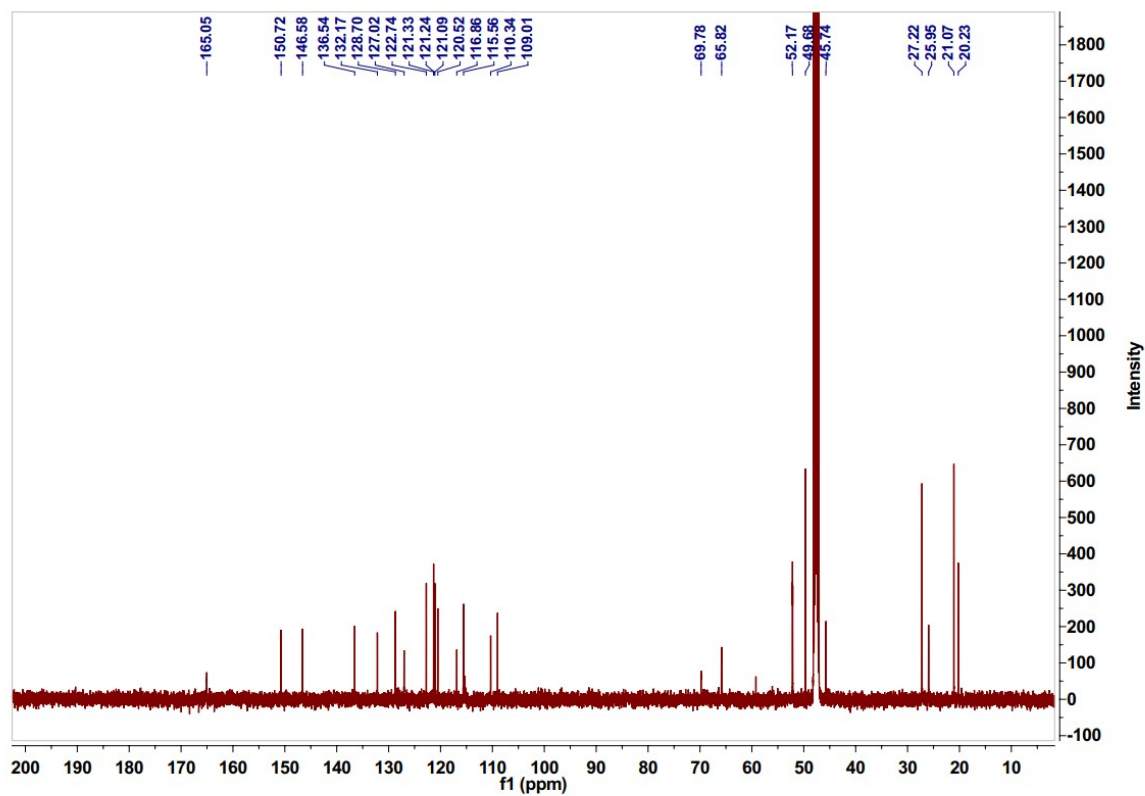


Fig. S2 $^{13}\text{C}\{^1\text{H}\}$ NMR spectrum of **JMT** in CD_3OD

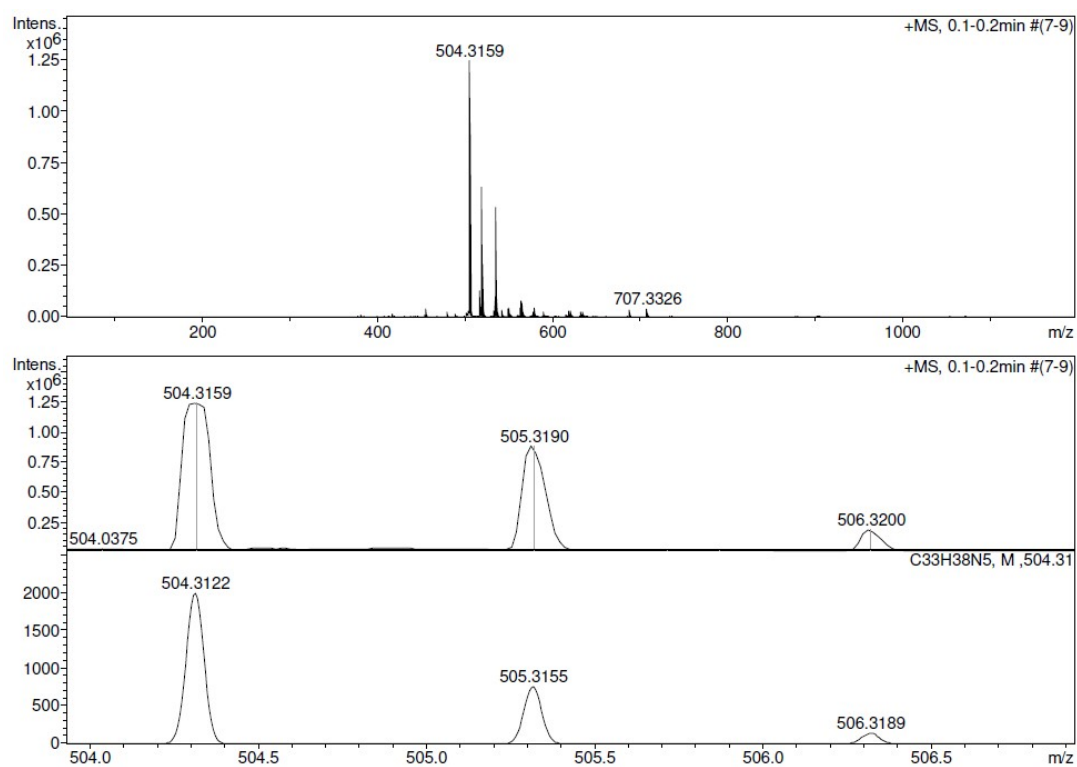


Fig. S3 ESI-HRMS mass spectrum of compound **JMT** calculated mass = 504.3122 Da, obtained mass = 504.3159 Da

Photophysical Properties

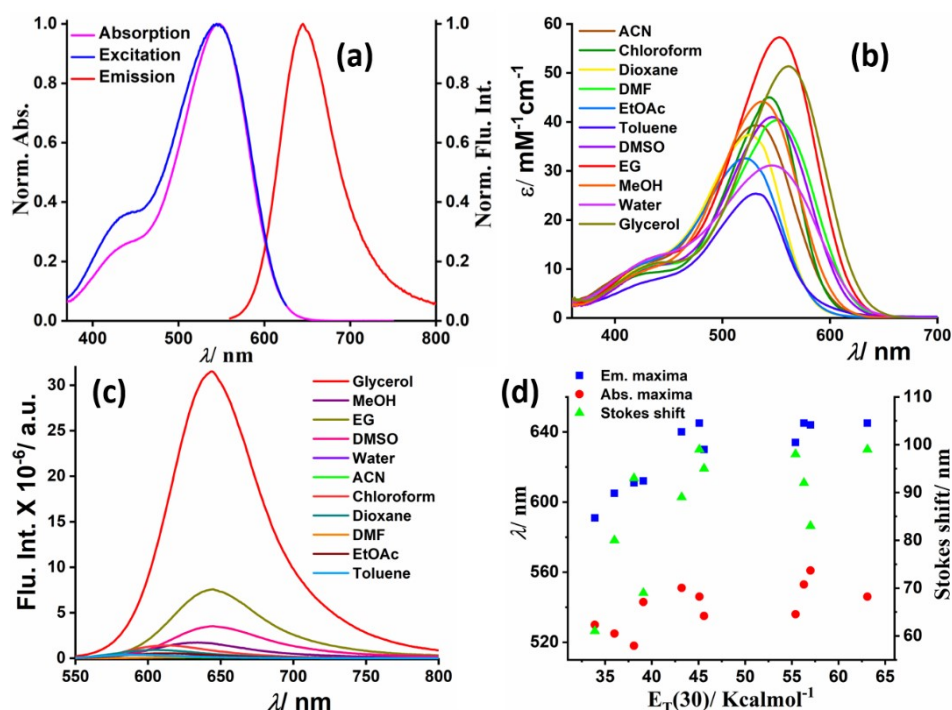


Fig. S4 (a) Absorbance ($\lambda_{\max} = 545$ nm), emission ($\lambda_{\max} = 645$ nm, $\lambda_{\text{ex}} = 545$ nm), and excitation ($\lambda_{\max} = 545$ nm, $\lambda_{\text{monitoring}} = 645$ nm) spectra of **JMT** in DMSO, (b) absorbance and (c) fluorescent spectra of **JMT** ($5 \mu\text{M}$) in different polar solvents, (d) maximum absorption wavelength, maximum fluorescent emission wavelength, and Stokes shift of **JMT** in different solvents; increasing polarity from left to right was plotted against their $E_T(30)$ values.

Table S1 Photophysical parameters of **JMT** in different polar solvents

Solvent	$\lambda_{\max}^{\text{abs.}}$ / nm	$\lambda_{\max}^{\text{em.}}$ / nm	Stokes shift / nm	Molar extinction coefficient / $\text{M}^{-1}\text{cm}^{-1}$	Rel. Q.Y. ^a
Water	546	645	99	31146	0.3
DMSO	546	645	99	41000	3.0
Methanol	536	634	98	44126	1.0
Ethylene Glycol	553	645	92	57272	4.0
Glycerol	561	644	83	51362	25.0

^a Relative quantum yield is measured using Nile red (QY = 0.7) as a standard (<https://www.photochemcad.com/databases/common-compounds/acridines/nile-red>, last accessed on 01.10.2023)

Table S2. Time-resolved fluorescence decay parameters for different water/glycerol mixture the decay times (τ_1 and τ_2), the respective fractional contributions (α_1 and α_2), the weighted average decay time (τ_{avg}) and the quality of fitting are shown (χ^2)

Viscosity (cP)	α_1	τ_1 (ns)	α_2	τ_2 (ns)	τ_{avg} (ns)	χ^2
45	33	0.2	67	0.5	0.4	1.2
80	35	0.2	65	0.7	0.6	1.2
156	28	0.3	72	1.0	0.9	1.2
346	25	0.6	75	1.4	1.2	1.3
905	23	0.8	77	1.7	1.6	1.2

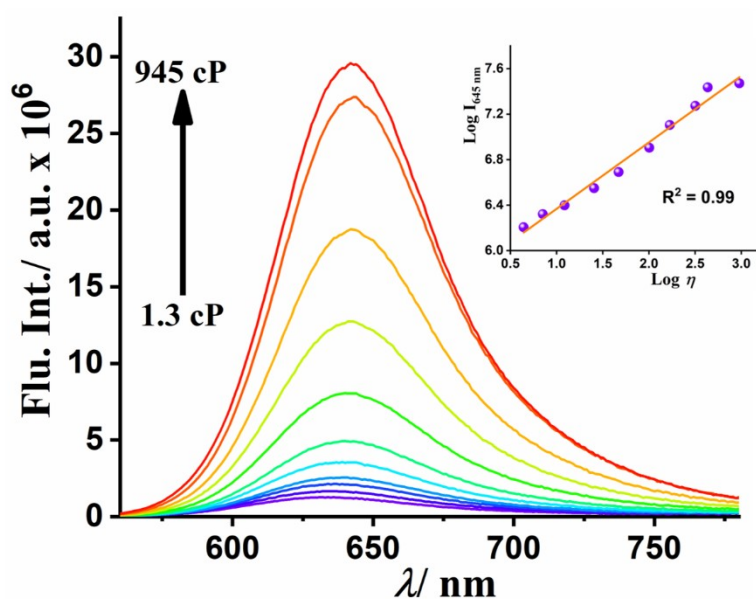


Fig. S5 Fluorescence emission plot of JMT with increasing viscosity using different methanol-glycerol mixtures. Inset: Double logarithmic scatter plot of fluorescence intensity vs. viscosity (cP) fitted according to Förster Hoffmann equation.

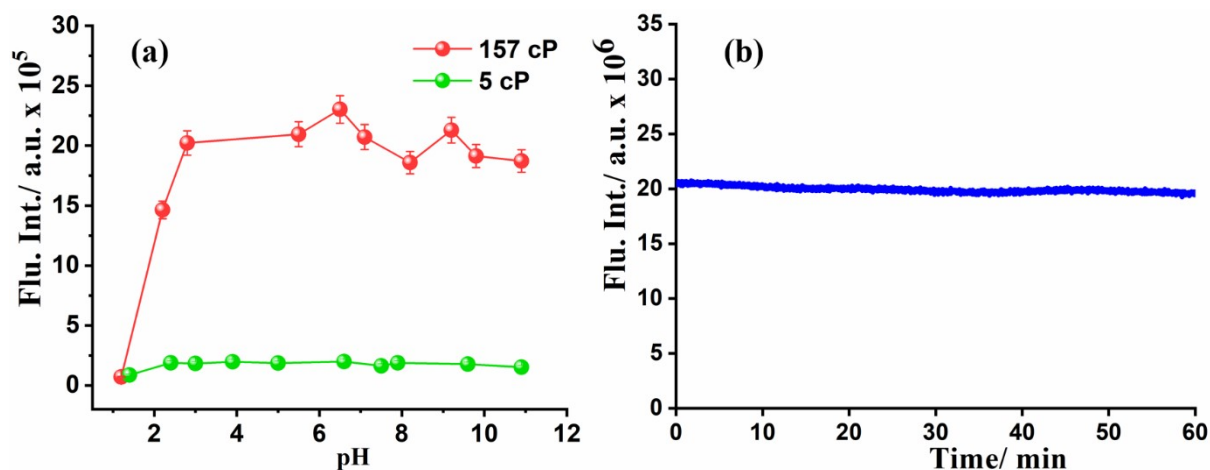


Fig. S6. (a) Scatter plot representing pH-dependent fluorescence intensity of **JMT** in water glycerol mixture with low and high viscosity, (b) fluorescence intensity of **JMT** in 95% glycerol water mixture monitored with time under continuous irradiation using Xenon lamp with 90 lx.

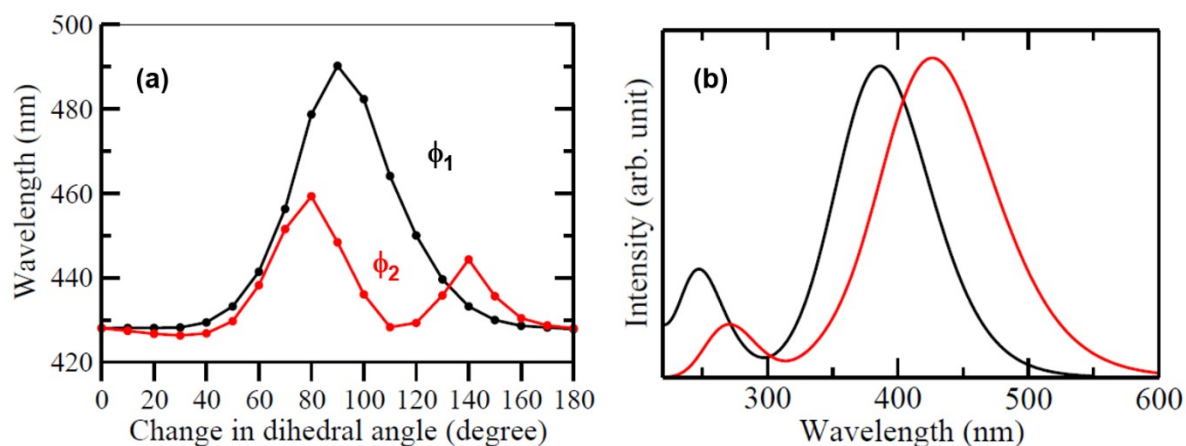


Fig. S7. (a) Variation of emission wavelength with dihedral angles ϕ_1 (black) and ϕ_2 (red), (b) computed absorption (black) and emission (red) spectra of modelled **JMT** molecule in gas phase.

Cytotoxicity and Live cell imaging application

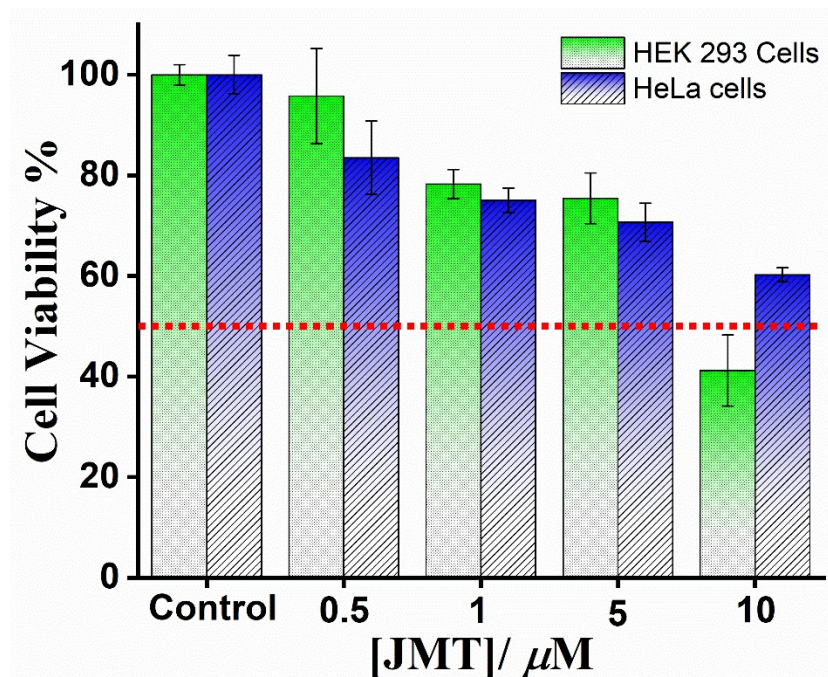


Fig. S8 MTT assay of the probe in HeLa cells (cancer cells) and HEK 293 cells (normal cells)

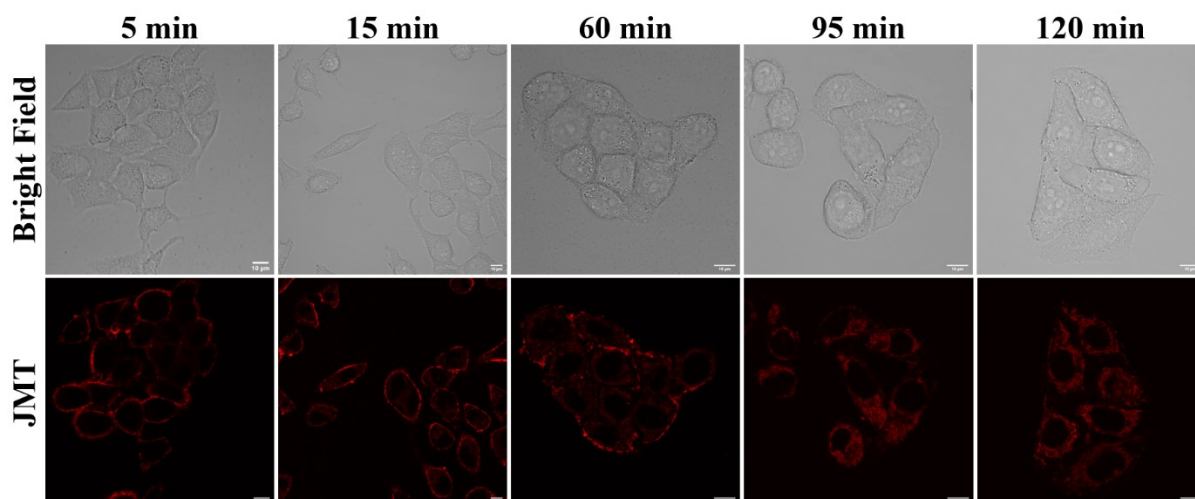


Fig. S9 Optimization of the incubation time: Confocal laser scanning microscopy images (CLSM) of HeLa cells incubated with JMT (0.5 μM) for indicated time points at 37 °C indicating saturation of fluorescence from JMT ($\lambda_{\text{ex}} = 561 \text{ nm}$, $\lambda_{\text{em}} = 570\text{-}670 \text{ nm}$) in 120 min. Scale bar = 10 μm.

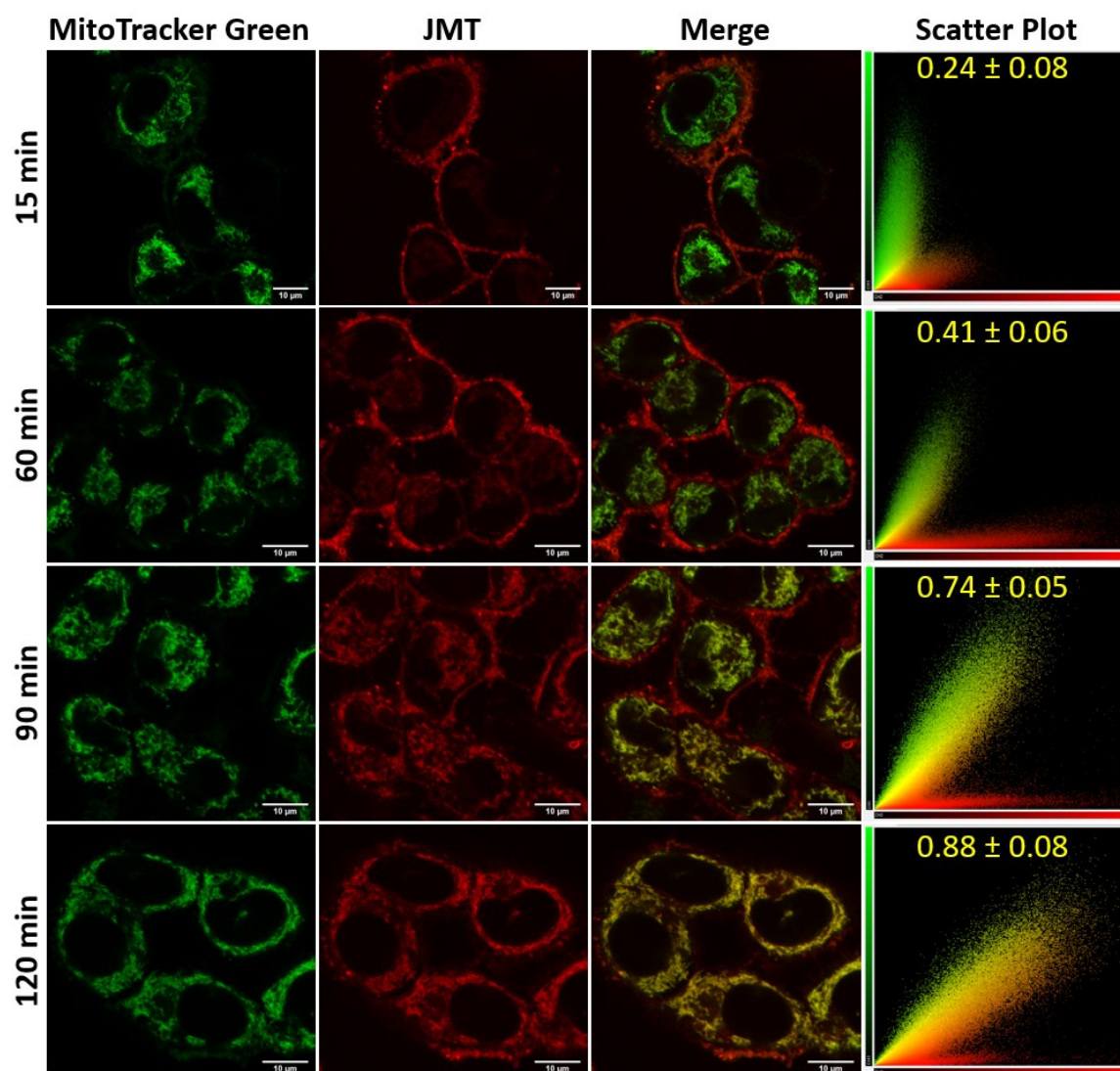


Fig. S10. (a) CLSM images of HeLa cells incubated with **JMT** ($0.5 \mu\text{M}$ for indicated time period, excitation wavelength of laser = 561 nm, emission collected = 570-670 nm) and subsequently with MitoTracker Green ($0.3 \mu\text{M}$, excitation wavelength of laser = 488 nm, emission collected = 500-530 nm) for 15 min at 37°C , third column is merged image of the green and red channel, and last column representing the scatter plot of green and red channel with obtained PCC value, Scale bar = $10 \mu\text{m}$

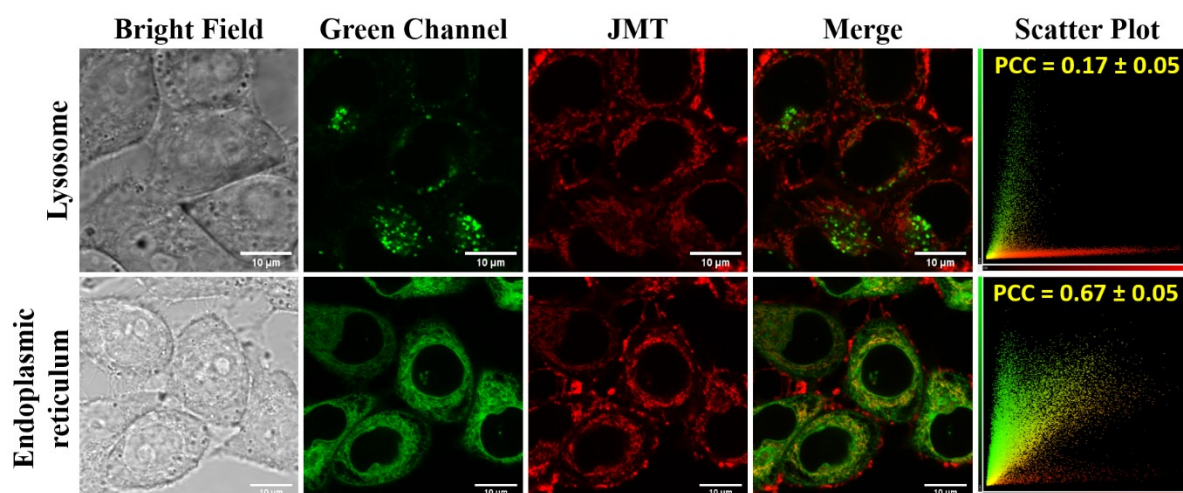


Fig. S11 Confocal laser scanning microscopy images (CLSM) of HeLa cells incubated with **JMT** ($0.5 \mu\text{M}$) for 2 h and subsequently with commercially available tracker ($0.3 \mu\text{M}$) for 15 min at 37°C . First column depicts the bright field, green channel and red channel representing fluorescence from commercially available tracker ($\lambda_{\text{ex}} = 488 \text{ nm}$, $\lambda_{\text{em}} = 500\text{-}530 \text{ nm}$) and **JMT** ($\lambda_{\text{ex}} = 561 \text{ nm}$, $\lambda_{\text{em}} = 570\text{-}670 \text{ nm}$), respectively, the fourth column is merged image of green and red channel, and last column representing the scatter plot of green and red channel with calculated Pearson's correlation coefficient (PCC) value. The top panel depicts fluorescence from LysoTracker Green and **JMT** and ER Tracker green and **JMT** (bottom panel). Scale bar = $10 \mu\text{m}$.

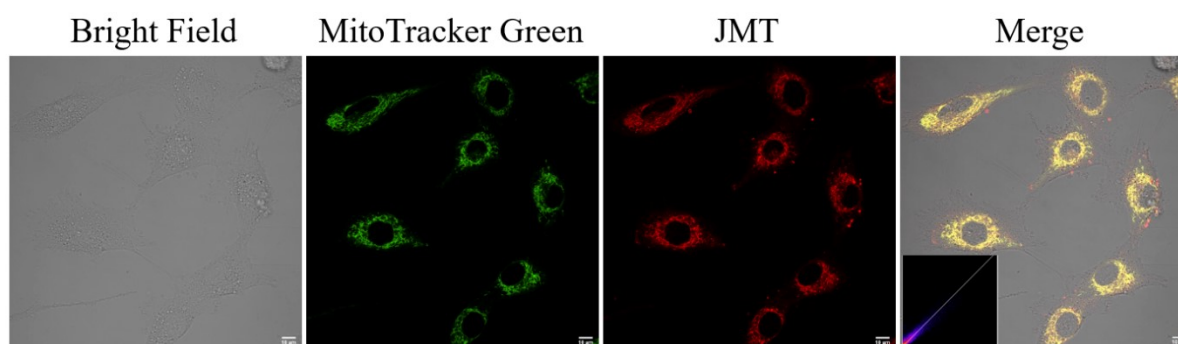


Fig. S12 U-87MG cells incubated with **JMT** ($0.5 \mu\text{M}$) for 2 h and subsequently with commercially available MitoTracker Green ($0.3 \mu\text{M}$) for 15 min at 37°C . CLSM images representing localization in mitochondria. Green channel ($\lambda_{\text{ex}} = 488 \text{ nm}$, $\lambda_{\text{em}} = 500\text{-}530 \text{ nm}$), red channel ($\lambda_{\text{ex}} = 561 \text{ nm}$, $\lambda_{\text{em}} = 570\text{-}670 \text{ nm}$), and merge of bright field, green, and red channel. Inset showing scatter plot with PCC value of 0.89 ± 0.04 . Scale bar = $10 \mu\text{m}$

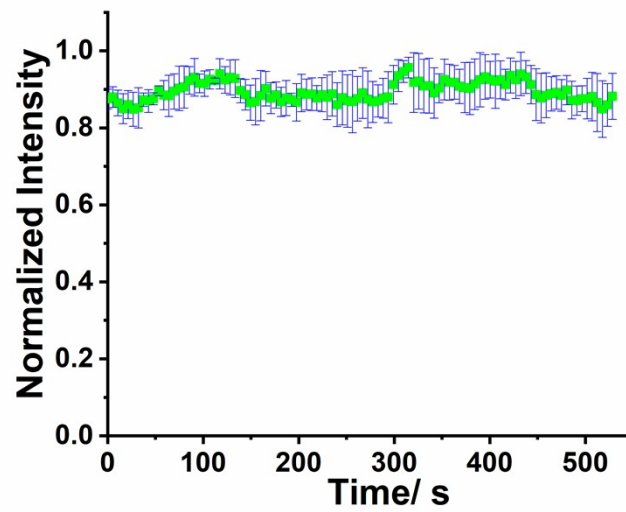


Fig. S13 Photostability of **JMT** inside the live HeLa cells monitored under continuous irradiation using a live-cell imaging condition.

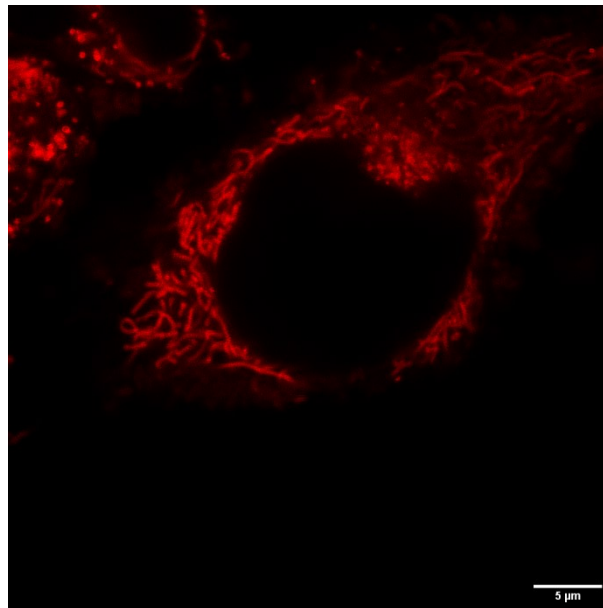


Fig. S14 Super-resolution confocal microscopy fluorescent images of HeLa cells stained with 0.5 μM **JMT** ($\lambda_{\text{ex}} = 561 \text{ nm}$, $\lambda_{\text{em}} = 570\text{-}670 \text{ nm}$). Super-resolution image was obtained with FV-OSR super-resolution system (Olympus) in conjunction with the FV3000 system. Scale bar = 5 μm

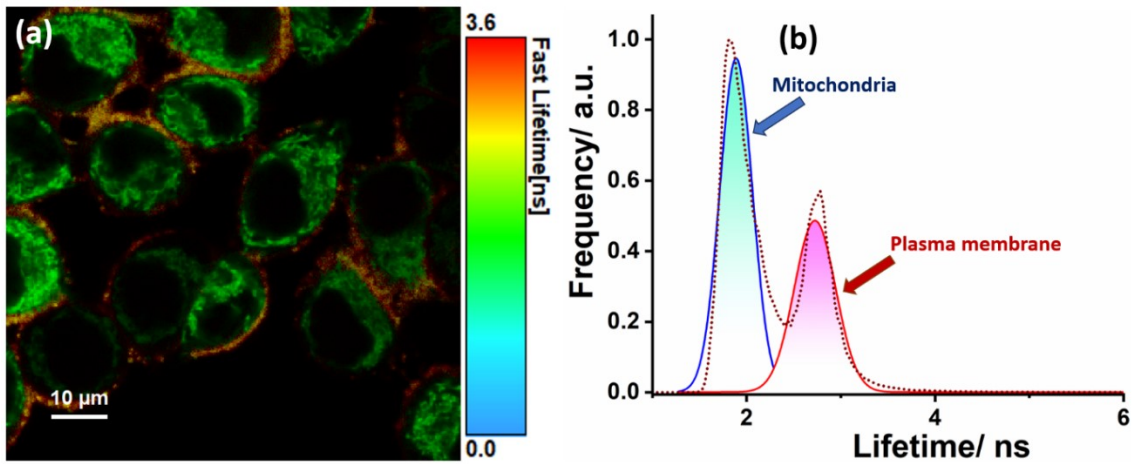


Fig. S15. (a) FLIM images of HeLa cells incubated with $0.5 \mu\text{M}$ **JMT** for 1 h, Scale bar = $10 \mu\text{m}$, (b) lifetime distribution of **JMT** in cells deconvoluted into two distributions of lifetimes from mitochondria and plasma membrane.

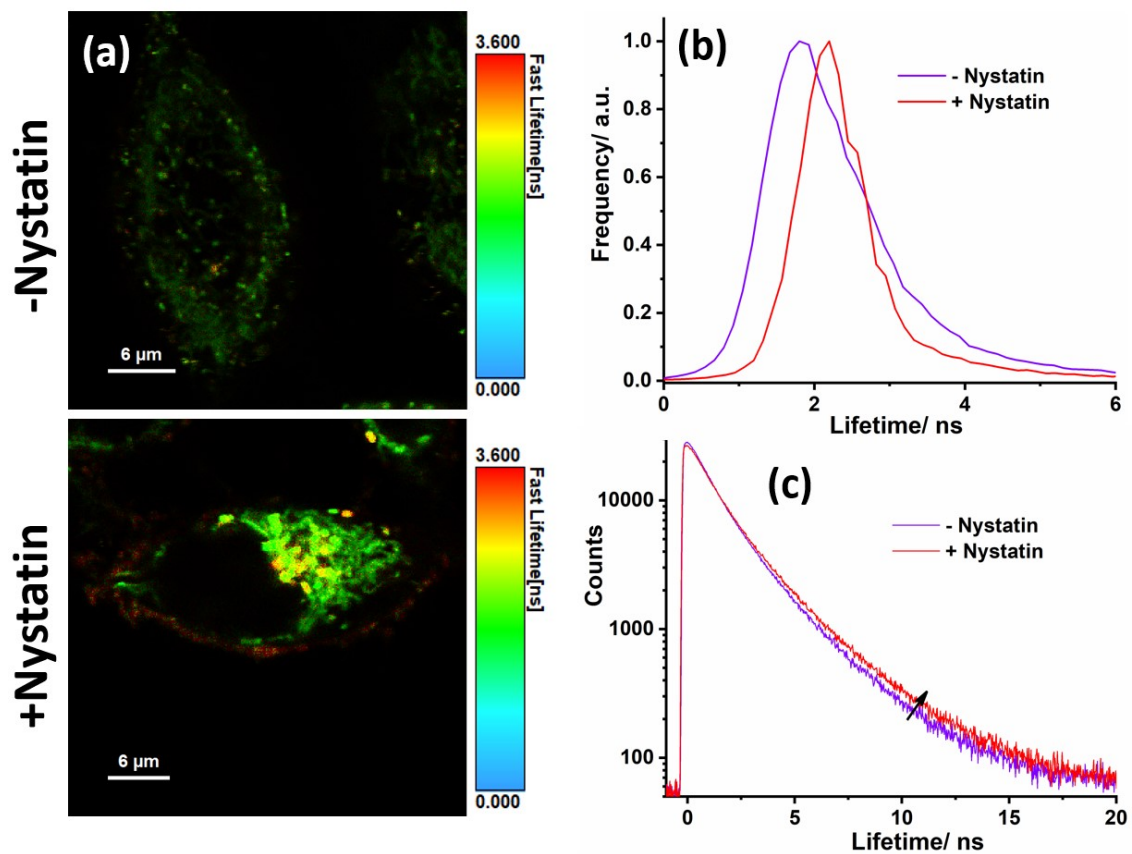


Fig. S16. (a) Fluorescence lifetime images of the HeLa cells stained with **JMT** for 2 h then treated with $10 \mu\text{M}$ nystatin for 30 min, (b) lifetime distribution of **JMT** in the histogram depicted increase in viscosity with nystatin treatment, (c) fluorescence decay plot also showing increase in lifetime after nystatin treatment.

Table S3. Time-resolved fluorescence decay parameters obtained from FLIM data before and after treatment of HeLa cells with nystatin the decay times (τ_1 and τ_2), the respective fractional contributions (α_1 and α_2), and the quality of fitting are shown (χ^2)

Treatment	α_1	τ_1 (ns)	α_2	τ_2 (ns)	χ^2
- Nystatin	36	2.3	63	1.0	1.2
+ Nystatin	12	3.5	87	1.2	1.3

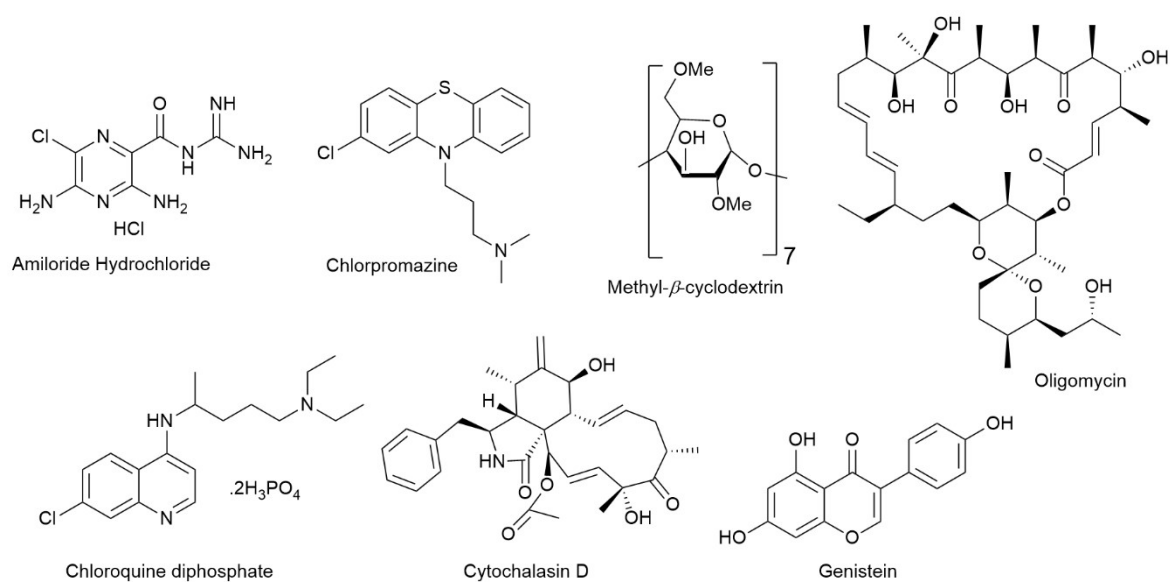


Fig. S17 Structures of the inhibitors used for cellular internalization mechanism.

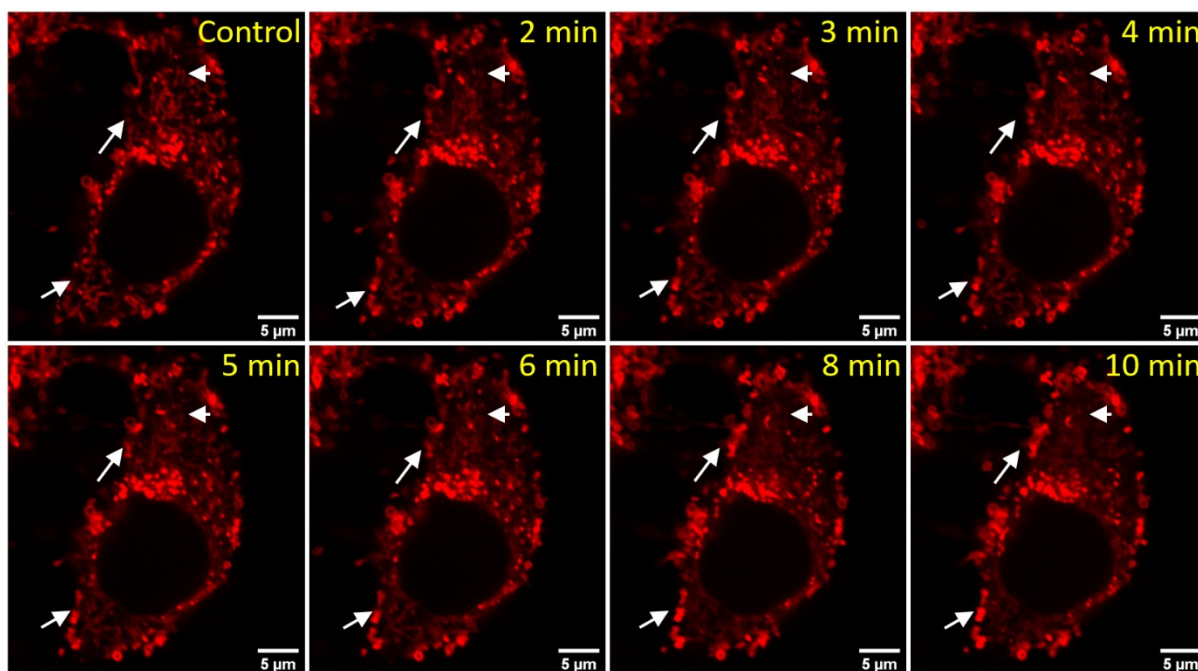


Fig. S18. CLSM images of HeLa cells incubated with **JMT** ($0.5 \mu\text{M}$, excitation wavelength of laser = 561 nm, emission collected = 570-670 nm) for 2 h and subsequently treated with CCCP ($20 \mu\text{M}$) for indicated time points at 37°C , demonstrating relocation of **JMT** from mitochondria to the plasma membrane, short arrow indicating mitochondria and long arrow indicating plasma membrane, Scale bar = $5 \mu\text{m}$

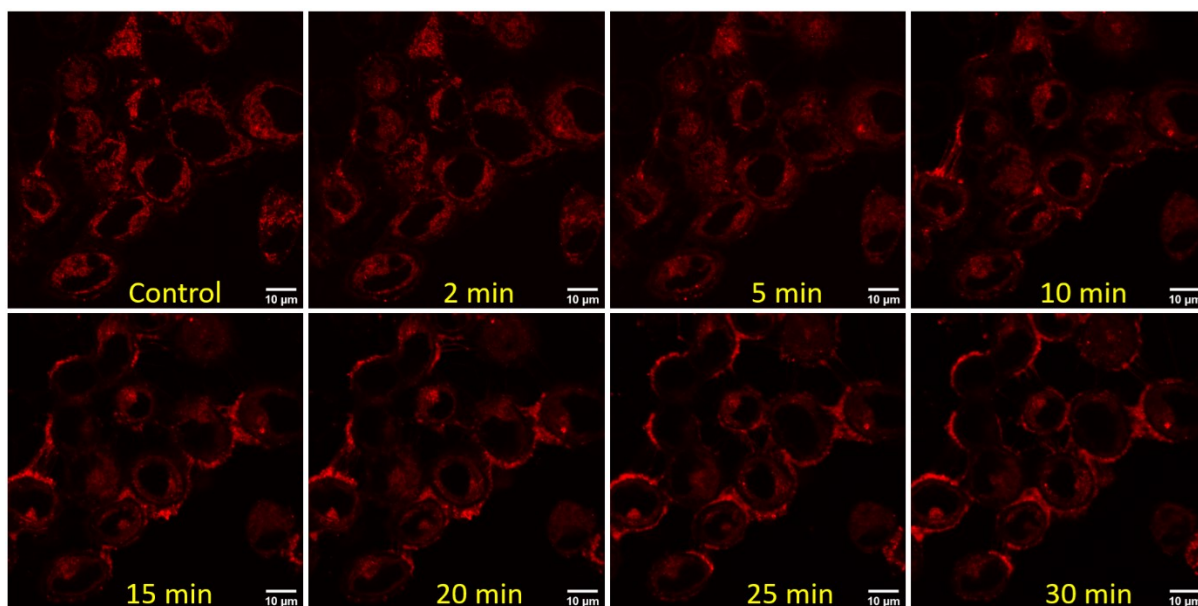


Fig. S19. CLSM images of HeLa cells incubated with **JMT** ($0.5 \mu\text{M}$, excitation wavelength of laser = 561 nm, emission collected = 570-670 nm) for 2 h and subsequently treated with valinomycin ($1 \mu\text{M}$) for indicated time points at 37°C , demonstrating relocation of **JMT** from mitochondria to the plasma membrane, Scale bar = $10 \mu\text{m}$

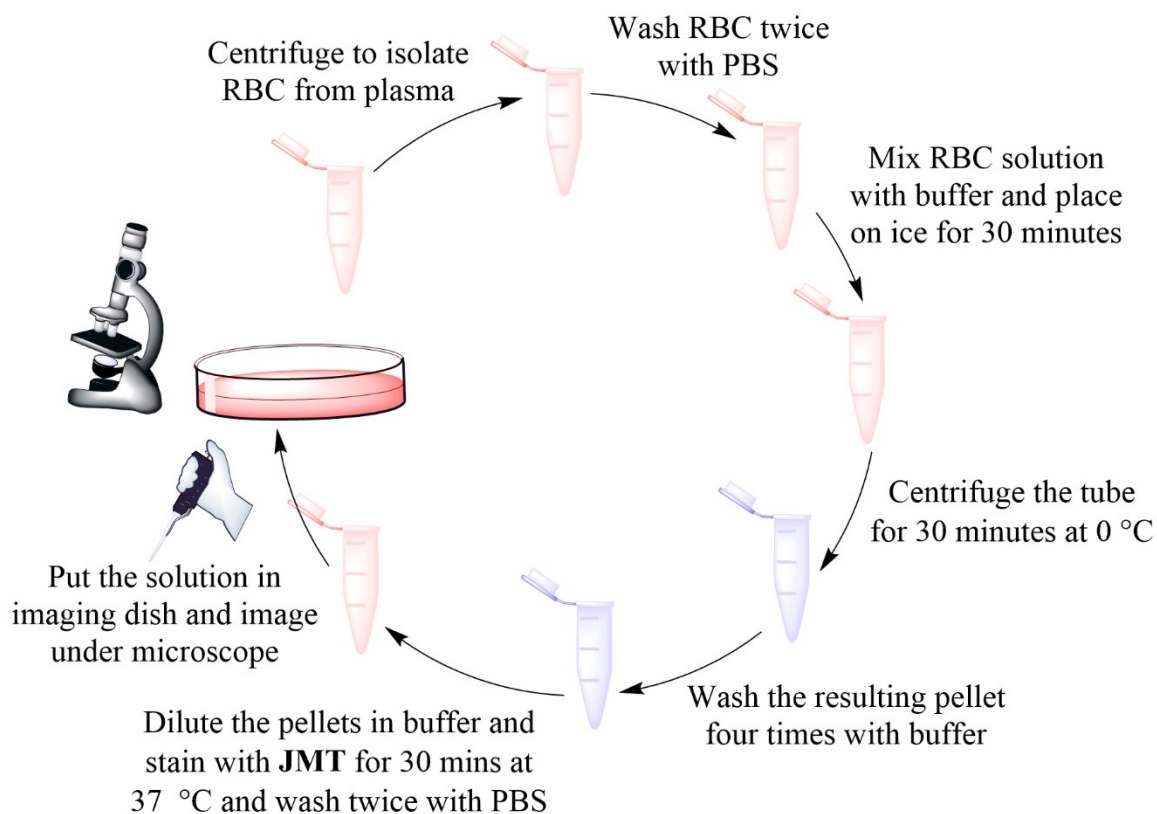


Fig. S20 Schematic representation of the separation of RBC ghost cells from the blood.

References

1. A. Silswal, A. Kanojiya and A. L. Koner, *Front. Chem.*, 2022, **10**, 1-9.